JMEPEG (2009) 18:1133–1139
DOI: 10.1007/s11665-008-9344-z

©ASM International
1059-9495/$19.00

# Intermetallic Compounds Formed in In-3Ag Solder BGA Packages with ENIG and ImAg Surface Finishes

**T.H. Chuang, C.C. Jain, and S.S. Wang**

(Submitted June 11, 2008; in revised form December 2, 2008)

**During the reflow process of In-3Ag solder ball grid array (BGA) packages with electroless nickel immersion gold (ENIG) and immersion silver (ImAg) surface finishes, continuous $(Au_{0.9}Ni_{0.1})In_2$ and scallop-shaped $(Ag_{0.9}Cu_{0.1})In_2$ intermetallic layers form at the interfaces of In-3Ag solder with Au/Ni/Cu and Ag/Cu pads, respectively. The $(Au_{0.9}Ni_{0.1})In_2$ layer breaks into clusters with increases in the aging time and temperature. Aging at 115 °C results in the formation of an additional continuous $Ni_{10}In_{27}$ layer on the Ni/Cu pads and the migration of $(Au_{0.9}Ni_{0.1})In_2$ intermetallic clusters into the solder matrix. In contrast, the $(Ag_{0.9}Cu_{0.1})In_2$ scallops grow into a continuous layer after aging treatment. Accompanying the interfacial reactions, $AgIn_2$ precipitates in the interior of In-3Ag solder balls and coarsens during aging, causing the ball shear strengths of reflown ENIG (1.18 N) and ImAg (1.11 N)-surface-finished solder joints to decrease gradually. However, the migration of $(Au_{0.9}Ni_{0.1})In_2$ clusters into the solder matrix of ENIG-surface-finished In-3Ag packages leads to an increase in their ball shear strengths after aging at 115 °C over 300 h. Both the ENIG- and ImAg-surface-finished In-3Ag solder joints, after ball shear tests, have fractured across the solder balls with ductile characteristics.**

**Keywords** ENIG, ImAg, In-3Ag solder, intermetallic compounds

## 1. Introduction

In response to the trend toward green products in the electronics industry, many efforts have been made to develop Pb-free solders, with eutectic Sn-Ag appearing as a promising alloy (Ref 1, 2). Compared to Sn-based solders, In-based solders possess advantages such as lower melting points, better wettability, and longer fatigue life (Ref 3, 4). Therefore, In-Ag solders have also been favored in specific applications for bonding temperature sensitive devices such as LEDs or thermal inductive sensors. However, few studies on In-Ag solders can be found in the literature. Chen et al. (Ref 5) investigated the melting and solidification characteristics of In-Ag solders through DSC analysis. Humpston et al. have also compared the spreading and joint-filling behavior of In-3Ag solder with those of other solder alloys on Au-deposited glass substrates (Ref 6). In addition, the interfacial reactions between liquid In-10Ag solders and Ag substrates, which lead to the formation of $AgIn_2$ intermetallics at the interface, have been analyzed by Liu and Chuang (Ref 7).

ENIG process is a popular surface-finishing process for Cu pads. The precious Au thin film acts as an oxidation protective layer and wetting layer for the Cu pads, and the Ni film acts as a barrier layer to prevent diffusion of the Cu out of the Au film. However, the Au surface finish often causes the formation of $AuSn_4$ intermetallic compounds and the embrittlement of solder joints, let alone the costly expense it entails (Ref 1). A recent alternative method for printed circuit board surface finishing involves immersion coating a 0.2-μm thick Ag film on the Cu pads (ImAg). The process takes only about 7 min, and the cost is nearly the same as that of traditional surface finishes involving Sn. In addition to the cost advantage, ImAg provides smooth surfaces and good wettability for liquid solder on Cu pads (Ref 2).

During the solder joint reflow process of solder joints on Au/Ni/Cu or Ag/Cu pads, the Au or Ag surface finish dissolves into the liquid solder, leading to the precipitation of intermetallic phases in the solder matrix or at the solder/pad interfaces. The solder alloy further reacts with the Ni layer or Cu pads, resulting in the formation of interfacial intermetallics. All of these intermetallics affect the bonding strength and material properties of the solder joints. It is also known that the resultant interfacial intermetallic layers can grow during the operation of electronic devices, which is also critical to the reliability of the packages. The effort of this study is thus concerned with the intermetallic compounds that form during the reflow and aging of In-3Ag solder BGA packages with ENIG and ImAg surface finishes. In these cases, liquid/solid and solid/solid reactions occur at the interfaces of In-3Ag solder with Au, Ag, Ni, and Cu layers. The influence of intermetallic reactions on the ball shear strength of solder joints has also been evaluated.

## 2. Experimental

The In-3Ag BGA packages with ENIG and ImAg surface finishes in this study contained 49 Cu pads with a thickness of 35 μm on each FR-4 substrate. For the ENIG process, the Cu pads were electroplated with 5-μm thick Ni and immersion plated with 0.7-μm thick Au. The ImAg-surface-finished Cu pads were immersion coated with 0.2-μm thick Ag film. In-3Ag

---

**T.H. Chuang, C.C. Jain,** and **S.S. Wang**, Department of Materials Science and Engineering, National Taiwan University, 1 Roosevelt Road, Sec. 4, Taipei 106, Taiwan. Contact e-mail: tunghan@ntu.edu.tw.

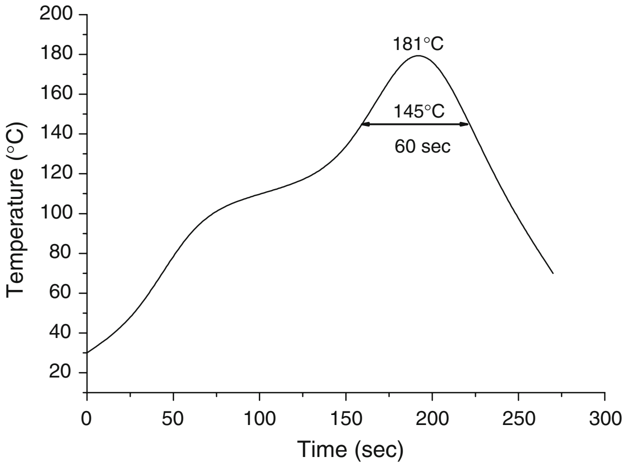

**Fig. 1** Temperature profile for reflowing of the In-3Ag BGA packages in this study

(wt.%) solder balls 0.4 mm in diameter were dipped in rosin mildly activated (RMA) flux, placed on the Au/Ni/Cu and Ag/Cu pads, and then reflown in a hot-air furnace equipped with five heating zones. Since the In-3Ag solder possesses a eutectic melting point at 144.85 °C, as analyzed by differential scanning calorimetry (DSC), the temperature profile for the reflow process shown in Fig. 1 contains a peak temperature of 180 °C and a melting time of 60 s. After reflow, certain specimens were further aged at 75 and 115 °C for various time periods ranging from 100 to 1000 h.

For the metallographic observations, the reflown and the aged specimens were cross sectioned through a row of solder balls, ground with 2000 grit SiC paper, and polished with 0.3-μm $Al_2O_3$ powder. The morphology of the intermetallic compounds in the solder matrix and at the solder/pad interface was observed by scanning electron microscope (SEM), and the chemical compositions of various intermetallic compounds were analyzed via an energy dispersive X-ray spectrometer (EDX) installed in the SEM. The bonding strengths of the In-3Ag solder balls on Au/Ni/Cu and Ag/Cu pads after reflow and various aging processes were measured using ball shear tests according to the low-speed shear test condition of the JEDEC-JESD22-B117 standard (October 2006), for which the shear rate and shear height were set at 0.1 mm/s and 80 μm (about 1/4 of the reflown ball height), respectively. The fractography of the solder joints after ball shear tests were observed in the SEM for characterization of the failure modes.

## 3. Results and Discussion

After reflow, many $AgIn_2$ fine particles about 3 μm in size were dispersed in the interior of the solder balls in the ENIG-surface-finished In-3Ag packages, as shown in Fig. 2(a). In addition, a continuous thin layer of intermetallic compounds formed at the In-3Ag solder/Ni interface of the ENIG-surface-finished packages, as shown in Fig. 2(b). Ahead of the continuous intermetallic layer, many cluster-shaped intermetallics can also be observed. EDX analyses indicated that both the continuous intermetallic layer and the cluster-shaped intermetallics had similar compositions of $(Au_{0.9}Ni_{0.1})In_2$. In contrast, the as-reflown ImAg-surface-finished specimens possessed scallop-shaped intermetallic compounds at the In-3Ag solder/Cu pad interface, as shown in Fig. 3(b). The chemical composition (at.%) of these intermetallic scallops, as analyzed with EDX, was Ag:Cu:In = 28.85:2.03:69.12, which corresponds to the $(Ag_{0.9}Cu_{0.1})In_2$ phase. Ahead of the $(Ag_{0.9}Cu_{0.1})In_2$ interfacial intermetallics, certain needle-shaped $AgIn_2$ can be observed. These $AgIn_2$ needles are the result of the new dissolution into the liquid solder of Ag film, which further reacts with the indium atoms in In-3Ag solder. Similar to the case of reflown ENIG-surface-finished packages, many $(Ag, Cu)In_2$ fine particles were dispersed in the interior of the solder ball, as shown in Fig. 3(a). EDX analyses indicate that the chemical composition (at.%) of these intermetallic particles is Ag:Cu:In = 21.35:13.41:65.24, which corresponds to the $(Ag_{0.6}Cu_{0.4})In_2$ phase. The lower Ag content in the $(Ag, Cu)In_2$ particles in the interior of solder ball compared with the intermetallic layer at the solder/pad interface implies that a certain amount of Ag film was left on the ImAg-surface-finished Cu pads after reflowing.

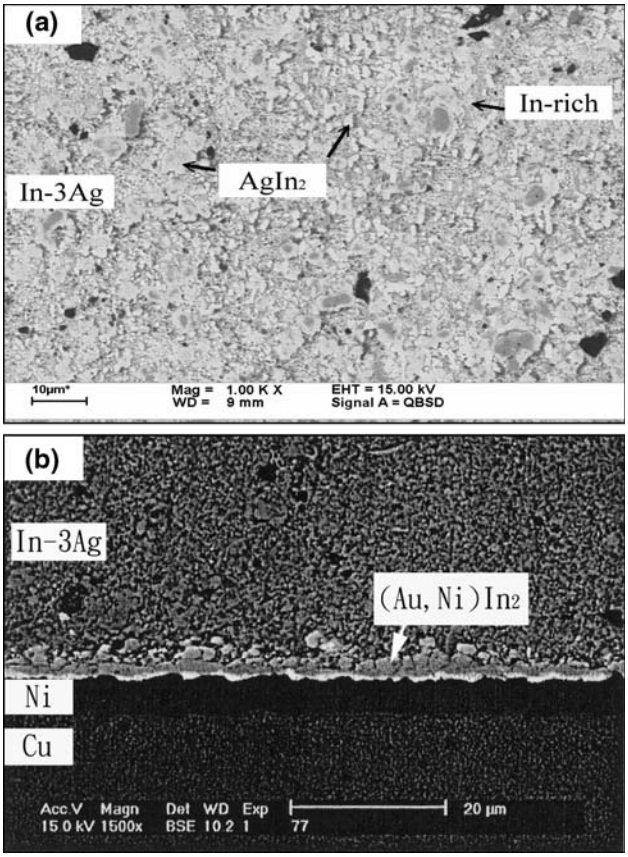

**Fig. 2** Morphology of intermetallic compounds formed after reflowing the In-3Ag solder balls on Au/Ni/Cu: (a) solder matrix and (b) solder/pad interface

Further aging of the ENIG-surface-finished In-3Ag BGA packages at 75 °C, as shown in Fig. 4, reveals that the $AgIn_2$ fine particles still exist in the interior of the solder ball and that the continuous $(Au_{0.9}Ni_{0.1})In_2$ intermetallic layer has been broken into clusters. However, the composition of these intermetallic clusters aged at 75 °C remains almost unchanged. In addition, certain intermetallic clusters have migrated into the solder matrix. Raising the aging temperature to 115 °C results

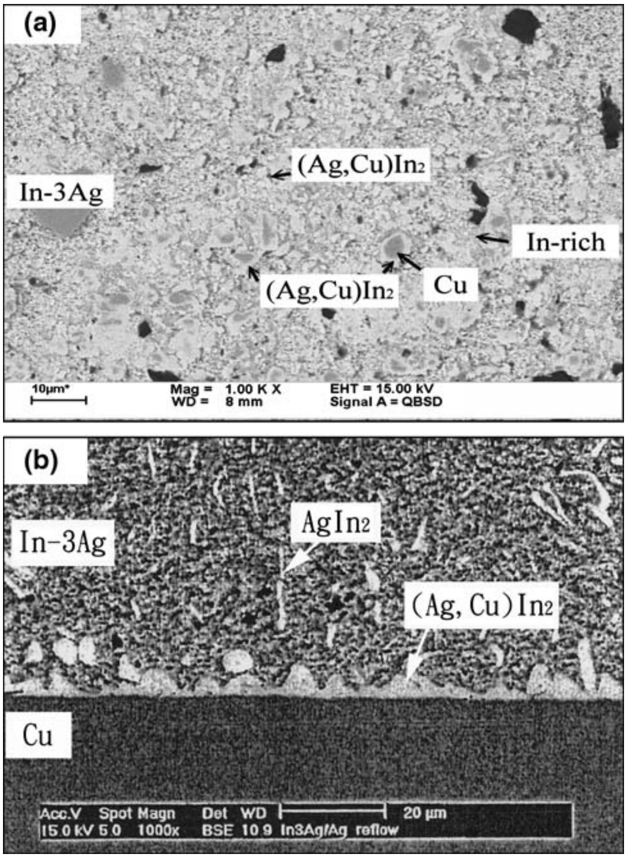

**Fig. 3** Morphology of intermetallic compounds formed after reflowing the In-3Ag solder balls on Ag/Cu: (a) solder matrix and (b) solder/pad interface

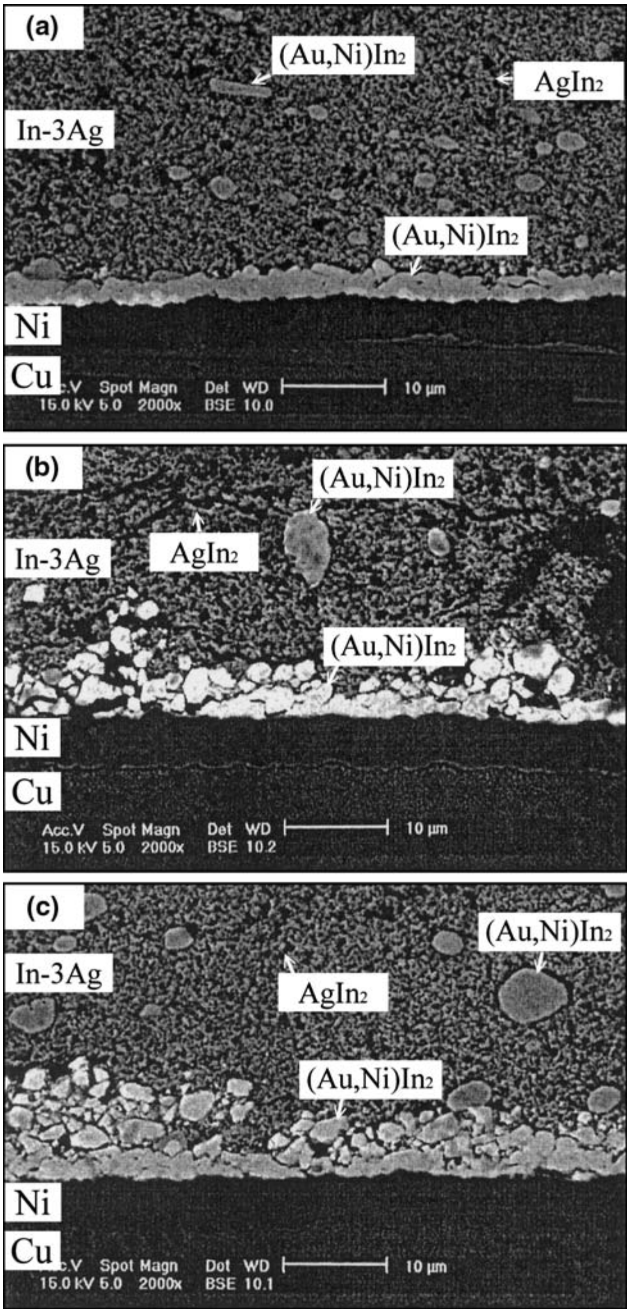

**Fig. 4** Morphology of intermetallic compounds formed in the In-3Ag BGA packages with Au/Ni/Cu pads after aging at 75 °C for various time periods: (a) 100 h, (b) 1000 h, and (c) 1500 h

in the formation of a new intermetallic layer between the $(Au_{0.9}Ni_{0.1})In_2$ clusters and Ni/Cu pads, as shown in Fig. 5. The composition (at.%) of this intermetallic interlayer is Ni:In = 29.22:70.78, which corresponds to the $Ni_{10}In_{27}$ phase. Figure 5 also shows that the $Ni_{10}In_{27}$ intermetallic layer grows as the aging time at 115 °C is increased. The formation of $Ni_{10}In_{27}$ intermetallics has also been reported by Chen and Lin for the liquid/solid interfacial reaction between eutectic In-49Sn solder and Ni substrate (Ref 8). However, they noticed that the $Ni_{10}In_{27}$ phase predominately appeared at temperatures higher than 275 °C, while another $Ni_2In_3$ intermetallic phase tended to form at temperatures lower than 275 °C. In contrast, Huang and Chen (Ref 9) found an $Ni_3Sn_4$ intermetallic phase at the interfaces of In-48$Sn_{(l)}$/$Ni_{(s)}$ couples after soldering reactions at 160 and 240 °C. In fact, a ternary $Ni_{33}In_{20}Sn_{47}$ phase has been reported in our previous study (Ref 10) for the In-49$Sn_{(l)}$/$Ni_{(s)}$ interfacial reactions at temperatures ranging from 150 to 450 °C. The appearance of $Ni_{10}In_{27}$ intermetallics during the In-3Ag/Ni interfacial reactions at 115 °C in this ENIG-surface-finished package, contradicting results reported in the literature, can be attributed to the solid/solid reactions of In-based solder in the present case. Furthermore, the $(Au_{0.9}Ni_{0.1})In_2$ intermetallic clusters are observed to migrate into the solder ball after long-term aging at 115 °C on account of the insufficient cohesive strength between $(Au_{0.9}Ni_{0.1})In_2$ clusters and the $Ni_{10}In_{27}$ intermetallic layer. Figure 6 shows that accompanying the intermetallic reactions at the solder/pad interface, the $AgIn_2$ fine particles that initially appeared in the top region of the as-reflown In-3Ag solder ball have coarsened into huge clusters, with a size of about 10 μm, after aging at 115 °C. The absence of such coarsened $AgIn_2$ clusters near the solder/pad interface is attributed to the preferential consumption of indium atoms for the growth of $(Au_{0.9}Ni_{0.1})In_2$ intermetallics in this interfacial region.

In the case of the ImAg-surface-finished In-3Ag packages, Fig. 7 and 8 show that the aging processes at 75 and 115 °C cause the initially needle-shaped $AgIn_2$ precipitates near the solder/pad interface observed in Fig. 3 to become cluster-shaped, coarsening with the aging time. In addition, the scallop-shaped $(Ag_{0.9}Cu_{0.1})In_2$ intermetallics at the In-3Ag/Cu interface

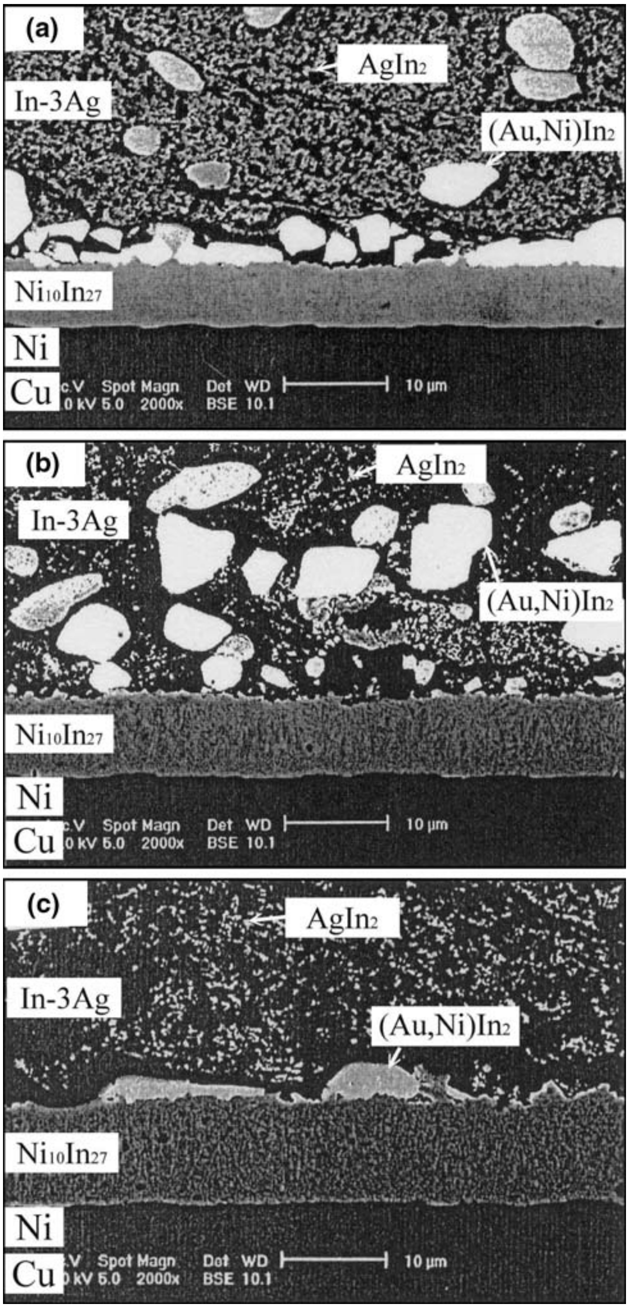

**Fig. 5** Morphology of intermetallic compounds formed in the In-3Ag BGA packages with Au/Ni/Cu pads after aging at 115 °C for various time periods: (a) 500 h, (b) 1000 h, and (c) 1500 h

of the as-reflown ImAg-surface-finished specimens become a smooth intermetallic layer that grows with the increase of the aging time and aging temperature, as shown in Fig. 7 and 8. In correspondence to the growth of intermetallics, the Cu contents in the interfacial $(Ag_{0.9}Cu_{0.1})In_2$ intermetallic layer increase from 2.03 at.% in the reflown state to 11.74 at.%, and then to 16.86 at.% when the specimens are aged at 75 °C with increases of the aging time from 0 h (as-reflown) to 500 h and then to 1000 h. The Cu content in the 115 °C aged specimens also increase to 17.61 at.% and then to 19.41 at.% with increases in the aging time to 500 h and then to 1000 h. Figure 8(c) reveals that after aging at 115 °C for 1000 h, the interfacial (Ag, Cu)$In_2$ intermetallic layer has been broken up, and a thin interlayer has appeared between the (Ag, Cu)$In_2$ intermetallics and Cu pads. The composition (at.%) of this new intermetallic layer is Cu:Ag:In = 53.02:3.59:43.39, which corresponds to a $Cu_{11}In_7$ phase. This implies that the indium atoms in In-3Ag solder have diffused through the (Ag, Cu)$In_2$ intermetallic layer and reacted with the Cu pad. For the ImAg-surface-finished In-3Ag packages, Fig. 9 also shows that the $AgIn_2$ particles in the interior of the solder ball have coarsened into large clusters about 13 µm in size.

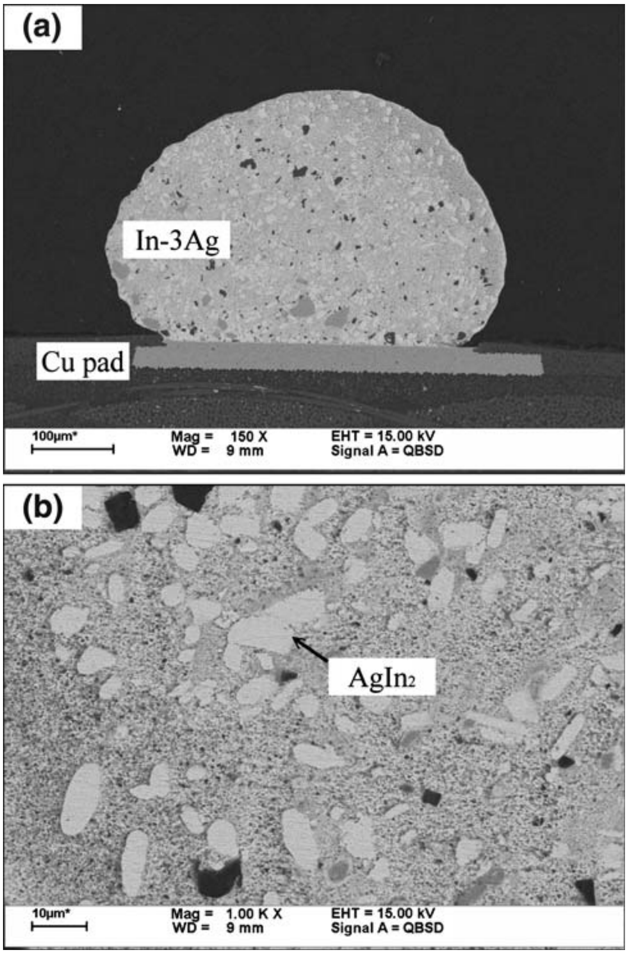

**Fig. 6** Coarsening of $AgIn_2$ particles in the interior of the solder ball for ENIG-surface finished In-3Ag package far from the solder/pad interface after aging at 115 °C for 100 h: (a) ENIG-surface finished In-3Ag BGA package and (b) solder matrix at the top of the solder ball

The ball shear strengths of ENIG- and ImAg-surface-finished In-3Ag BGA solder packages are shown in Fig. 10 and Table 1. Fractographic observations indicate that all the specimens, after ball shear tests, fracture across the solder balls with ductile characteristics. In Table 1, it can be seen that the solder joints in the reflown In-3Ag solder BGA packages with Au/Ni/Cu pads (ENIG) possess a strength of 1.18 N. Figure 10(a) shows that after aging at 75 and 115 °C for 100 h, the ball shear strengths have decreased to 1.11 and 0.92 N, respectively. With further increase of the aging time to over 700 h at 75 °C, the ball shear strengths drop gradually to values of about 0.82 N. However, aging at 115 °C for 300 h causes the ball shear strength to drop to a value of 0.76 N. In contrast,

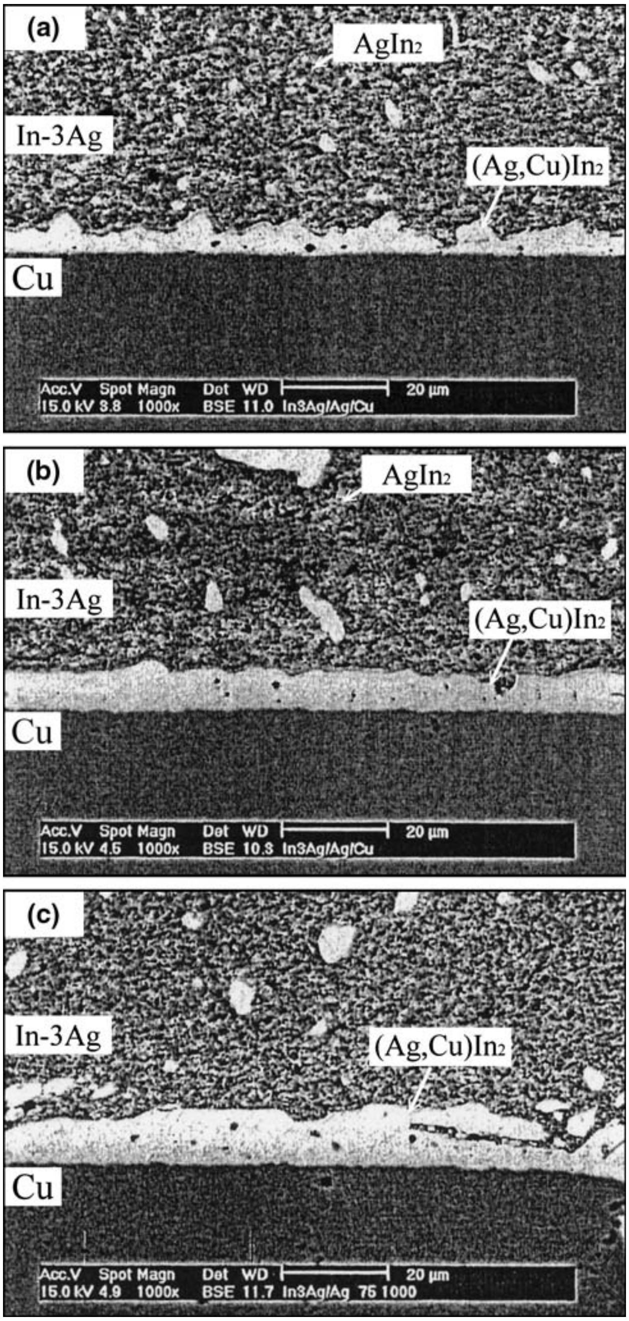

**Fig. 7** Morphology of intermetallic compounds formed in the In-3Ag BGA packages with Ag/Cu pads after aging at 75 °C for various time periods: (a) 100 h, (b) 500 h, and (c) 1000 h

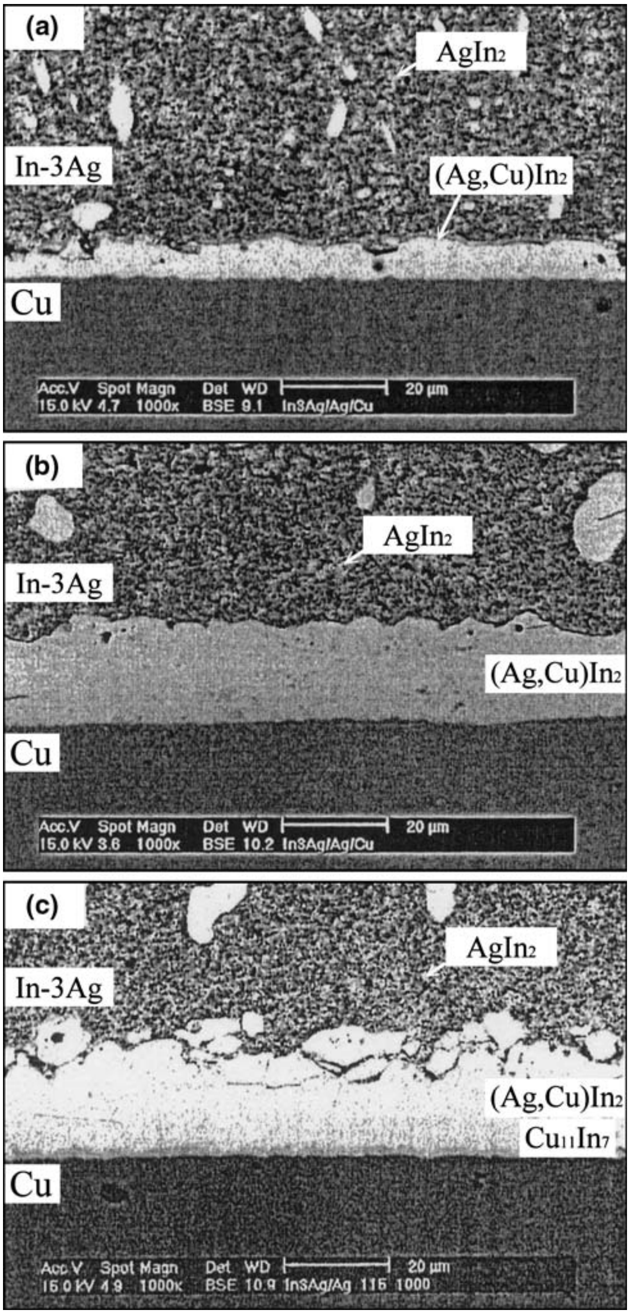

**Fig. 8** Morphology of intermetallic compounds formed in the In-3Ag BGA packages with Ag/Cu pads after aging at 115 °C for various time periods: (a) 100 h, (b) 500 h, and (c) 1000 h

Fig. 10(a) reveals that with a further increase of the aging time ranging from 300 to 1000 h, the bonding strengths gradually rise from 0.76 N to a value of 0.93 N. One possible explanation for this increase is that the $(Au_{0.9}Ni_{0.1})In_2$ intermetallics that migrate into the solder balls after long-term aging at 115 °C, as evidenced in Fig. 5, have a strengthening effect on the In-3Ag solder matrix. For the reflown ImAg-surface-finished In-3Ag packages, a bonding strength of 1.11 N is obtained, as shown in Table 1 and Fig. 10(b). After aging at 75 and 115 °C for 100 h, the ball shear strengths have dropped to 1.02 and 0.78 N, respectively. The bonding strengths further decrease continuously to 0.84 N and 0.59 N with an increase of the aging time to 1000 h at both 75 and 115 °C, respectively. The degradation of bonding strengths after aging treatments for ImAg-surface-finished In-3Ag solder joints could be caused by the softening of the solder matrix because of the coarsening of $AgIn_2$ precipitates, which was not compensated for by the other intermetallic phases, such as the $(Au_{0.9}Ni_{0.1})In_2$ in the ENIG-surface-finished packages. Figure 11 reveals that both the ENIG- and ImAg-surface-finished In-3Ag solder joints, after ball shear tests, have fractured across the solder balls with ductile characteristics. The existence of needle-shaped $AgIn_2$ precipitates in the solder matrix with Ag/Cu pads results in a galling wear surface as evidenced by the fractography

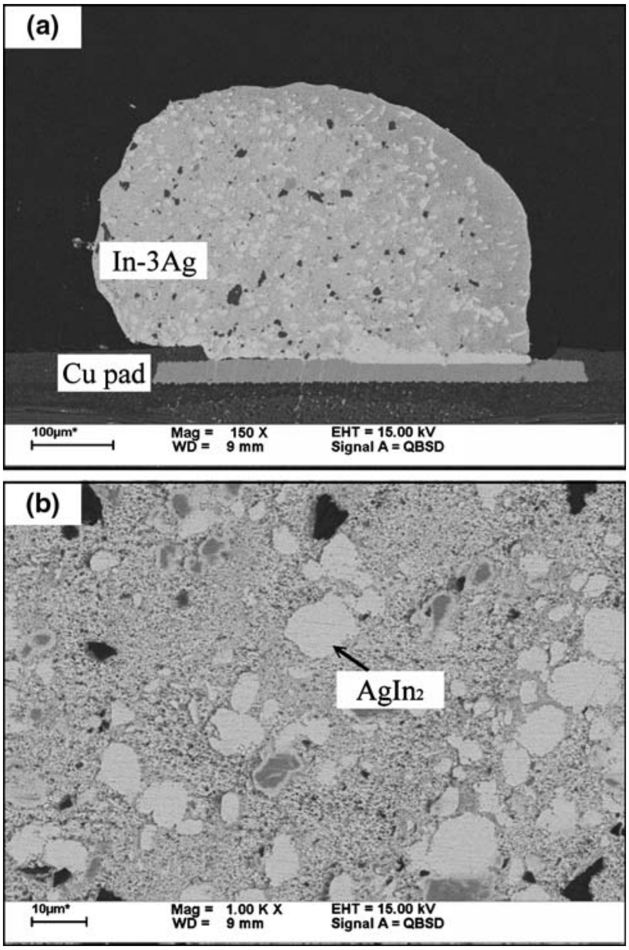

**Fig. 9** Coarsening of $AgIn_2$ particles in the interior of solder ball for ImAg-surface finished In-3Ag package far from the solder/pad interface after aging at 115 °C for 100 h: (a) ImAg-surface finished In-3Ag BGA package and (b) solder matrix at the top of the solder ball

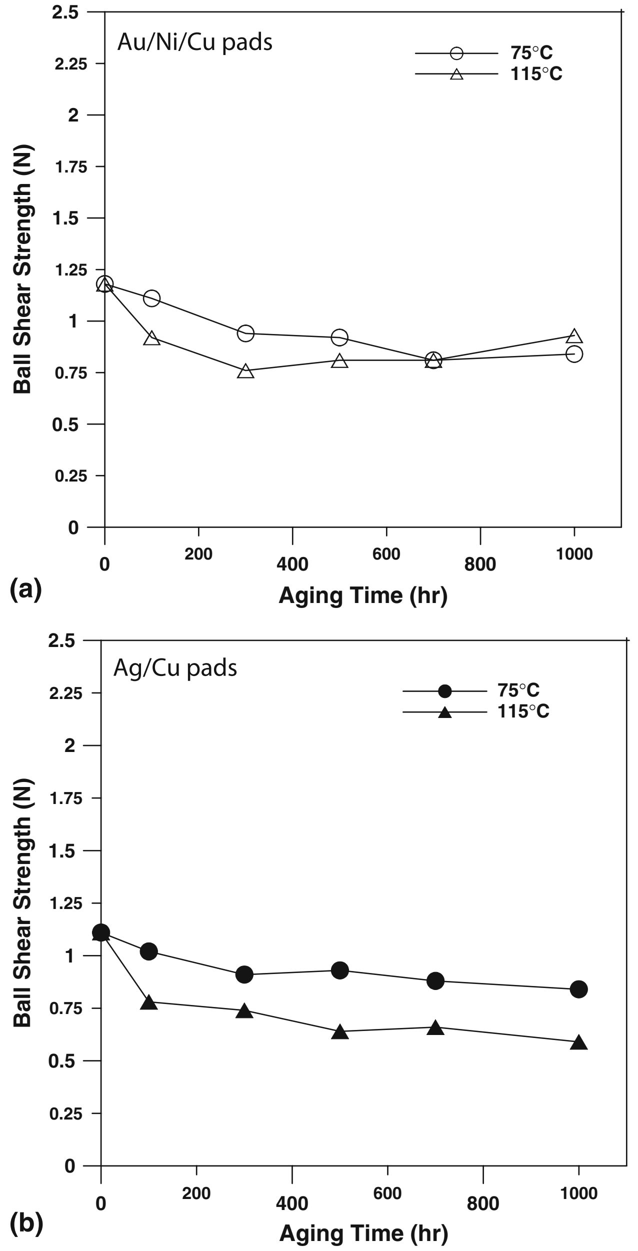

**Fig. 10** Ball shear strengths of the In-3Ag solder BGA packages with (a) Au/Ni/Cu and (b) Ag/Cu pads after aging at 75 and 115 °C for various time periods

**Table 1 Ball shear strengths of In-3Ag solder BGA packages with Au/Ni/Cu pads and Ag/Cu pads after aging at 75 and 115 °C for various time periods**

| | Au/Ni/Cu pads | | Ag/Cu pads | |
|---|---|---|---|---|
| Aging time | 75 °C | 115 °C | 75 °C | 115 °C |
| As-reflown | 1.18 N | 1.18 N | 1.11 N | 1.11 N |
| 100 h | 1.11 N | 0.92 N | 1.02 N | 0.78 N |
| 300 h | 0.94 N | 0.76 N | 0.91 N | 0.74 N |
| 500 h | 0.92 N | 0.81 N | 0.93 N | 0.64 N |
| 700 h | 0.81 N | 0.84 N | 0.88 N | 0.66 N |
| 1000 h | 0.82 N | 0.93 N | 0.84 N | 0.59 N |

(Fig. 11b). In contrast, a burnishing wear track morphology can be observed in Fig. 11(a) for the solder joints with Au/Ni/Cu pads.

## 4. Conclusions

It was the purpose of this study to investigate the intermetallic reactions and their effects on the bonding strengths of solder joints during reflow and aging in In-3Ag BGA packages with ENIG- and ImAg-surface finishes. Experimental results indicate that the intermetallic reactions occur at the interfaces of the In-3Ag solder with Au/Ni/Cu and Ag/Cu pads, leading to the formation of continuous $(Au_{0.9}Ni_{0.1})In_2$ and scallop-shaped $(Ag_{0.9}Cu_{0.1})In_2$ intermetallic layers, respectively. Further aging of the ENIG-surface-finished In-3Ag packages at 75 and 115 °C causes the continuous $(Au_{0.9}Ni_{0.1})In_2$ intermetallic layer to break into clusters. An extra $Ni_{10}In_{27}$ phase appears between the $(Au_{0.9}Ni_{0.1})In_2$ clusters and Ni layer after aging at 115 °C for 1000 h, which causes the $(Au_{0.9}Ni_{0.1})In_2$ clusters to be stripped away from the $Ni_{10}In_{27}$ intermetallic layer and migrate into the solder matrix. In

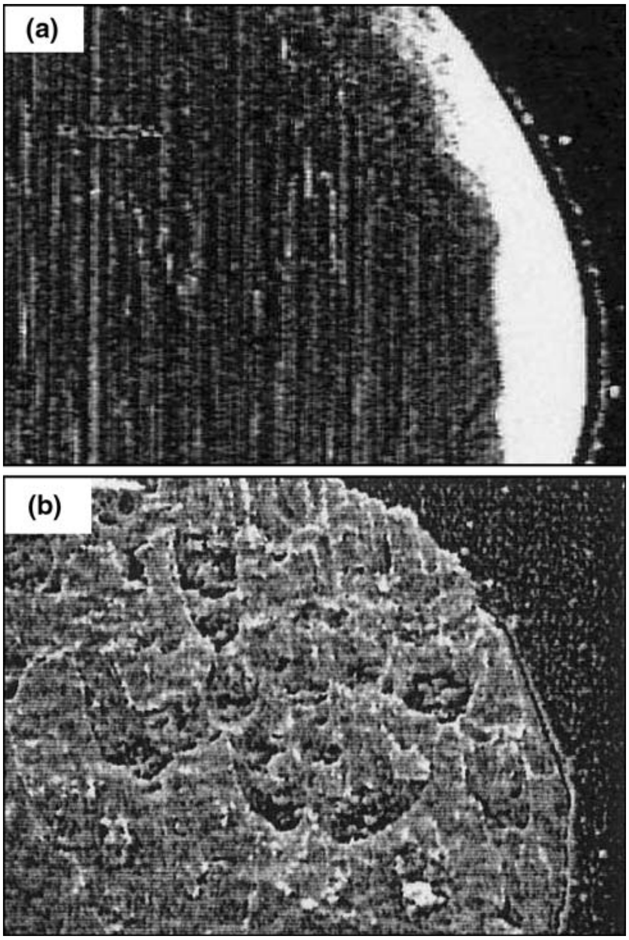

**Fig. 11** Fractography of as-reflown In-3Ag solder joints in BGA packages with (a) Au/Ni/Cu and (b) Ag/Cu pads after ball shear teats

contrast, the (Ag, Cu)$In_2$ intermetallic layer grows continuously during the aging process at 75 and 115 °C. Accompanying the intermetallic reactions at the solder/pad interfaces of ENIG- and ImAg-surface-finished In-3Ag BGA packages, the $AgIn_2$ fine precipitates that initially appear in the reflown solder matrix coarsen into intermetallic clusters after aging. This coarsening effect results in the softening of the solder matrix and the decrease of ball shear strengths from 1.18 and 1.11 N (in the reflown state) to about 0.82 and 0.84 N for the ENIG- and ImAg-surface-finished In-3Ag solder joints, respectively, after aging at 75 °C for 1000 h. However, the strengthening effect of the migration of $(Au_{0.9}Ni_{0.1})In_2$ clusters into the solder matrix of ENIG-surface-finished packages leads to the rise of their ball shear strengths after aging at 115 °C over 300 h.

## Acknowledgments

Sincere gratitude goes to National Taiwan University and the National Science Council, Taiwan, for sponsoring this research under Grants No. 96R0210 and No. NSC-96-2221-E002-150-MY3.

## References

1. D.M. Jacobson and G. Humpston, Gold Coatings for Fluxless Soldering, *Gold Bull.*, 1989, **22**, p 9–18
2. J.H. Lau, C.P. Wong, N.C. Lee, and S.W. Ricky Lee, *Electronics Manufacturing with Lead-Free, Halogen-Free Conductive-Adhesive Materials*, McGraw-Hill Handbooks, 2003
3. J. Glazer, Metallurgy of Low Temperature Pb-Free Solders for Electronics Assembly, *Int. Mater. Rev.*, 1995, **40**(2), p 65–93
4. K. Shimizu, T. Nakanishi, K. Karasawa, K. Hashimoto, and K. Niwa, Solder Joint Reliability of Indium-Alloy Interconnection, *J. Electron. Mater.*, 1995, **24**(1), p 39–45
5. S.W. Chen, C.C. Lin, and C.M. Chen, Determination of the Melting and Solidification Characteristics of Solders Using Differential Scanning Calorimetry, *Metall. Trans. A Phys. Metal. Mater. Sci.*, 1998, **29**, p 1965–1972
6. G. Humpston and D.M. Jacobson, The Relationship Between Solder Spread and Joint Filling, *GEC J. Res.*, 1991, **8**(3), p 145–150
7. Y.M. Liu and T.H. Chuang, Interfacial Reactions Between In-10Ag and Ag Substrates, *J. Electron. Mater.*, 2000, **29**(11), p 1328–1332
8. C.J. Chen and K.L. Lin, Wetting Interactions Between the Ni-Cu-P Deposit and In-Sn Solders, *IEEE Trans. Compon. Pack. Manuf. Technol. B: Adv. Pack.*, 1997, **20**, p 211–216
9. C.Y. Huang and S.W. Chen, Interfacial Reactions in In-Sn/Ni Couples and Phase Equilibria of the In-Sn-Ni System, *J. Electron. Mater.*, 2002, **31**(2), p 152–160
10. S.S. Wang, Y.H. Tseng, and T.H. Chuang, Intermetallic Compounds Formed During the Interfacial Reactions Between Liquid In-49Sn Solder and Ni Substrates, *J. Electron. Mater.*, 2006, **35**(1), p 165–169